Anesthesiology 2003; 98:209–16

Loss of T-type Calcium Current in Sensory Neurons of Rats with Neuropathic Pain

J. Bruce McCallum, Ph.D., Wai-Meng Kwok, Ph.D.,† Michelle Mynlieff, Ph.D.,‡ Zeljko J. Bosnjak, Ph.D.,§ Quinn H. Hogan, M.D.‖*

Background: **Pathophysiology in the primary sensory neuron may contribute to chronic neuropathic pain. Ca channels play a central role in neuronal processes, and sensory neurons are rich in low-voltage–activated calcium channels (LVACCs). However, the physiologic function of these channels is unknown. Their possible role in rebound burst firing makes them a candidate for increased excitability after neuropathic injury.**

Methods: **This study uses pharmacological methods to isolate LVACC in cells from the dorsal root ganglia of neuropathic and sham-operated rats, including the blockade of high-voltage–activated Ca channels with fluoride and selective toxins. LVACCs were examined with conventional whole cell patch clamp electrophysiology techniques.**

Results: **After chronic constriction injury of the peripheral axon, LVACC was significantly reduced compared to sham rats as shown by a 60% reduction in peak current density and an 80% reduction in total calcium influx. A depolarizing shift in the voltage dependence of activation and an increase in the rate of deactivation and inactivation appear to cause this reduction of LVACC. Either Ni^{2+} or mibefradil, blockers of LVACC, applied in the bath to normal dorsal root ganglion cells during current clamp significantly and reversibly increased excitability.**

Conclusions: **These results suggest that loss of LVACC may contribute to decreased spike frequency adaptation and increased excitability after injury to sensory neurons. Through decreased Ca^{2+} influx, the cell becomes less stable and more likely to initiate or transmit bursts of action potentials. Consequently, modulation of Ca^{2+} currents at the dorsal root ganglion may be a potential method of therapeutic intervention.**

CHRONIC pain incurred as a result of peripheral pathology or posttraumatic neuropathy is maladaptive, difficult to treat, and poorly understood at the cellular level. Multiple mechanisms likely contribute to neuropathic pain. Central sensitization[1–3] results from a cumulative process of polysynaptic facilitation triggered by increased firing from peripheral afferent pathways.[4] Animal studies replicating chronic pain have shown that heightened activity originating in the dorsal root ganglion (DRG) contributes to central sensitization,[5–8] even after complete ligation of nerves extending to cutaneous receptive fields.[9] Injury may thus transform a transient response to touch into a sustained, resonating response.[10,11] Increased subthreshold oscillations at the resting membrane potential may augment burst firing of sensory neurons.[12,13] Sustained afferent bombardment is a prelude to central sensitization by which the afferent signals are misinterpreted and amplified.[14]

Previous animal studies of sensory neurons have shown that the cell bodies of neurons having lightly myelinated Aδ fibers are rich in low-voltage–activated calcium channels (LVACCs),[15,16] which in other tissues have been implicated in increasing excitability, including rebound burst firing[17] and epilepsy.[18] Since high-frequency activity may contribute to central sensitization, an increase in LVACC would be a likely candidate for the current underlying spontaneous discharge in afferent pathways. However, the function of LVACC in the DRG is unclear. We previously reported that neuropathic injury reduced high-voltage–activated (HVA) calcium currents by about 30% in medium-sized, presumably Aδ neurons.[19] These findings have been partially duplicated in other studies.[20] We observed an apparent absence in low-voltage–activated, T-type calcium currents after injury, but we did not employ specific techniques to isolate these currents. Although no specific antagonist for these channels exists, they can be studied through the use of pharmacological and electrophysiological tools for eliminating high-voltage–activated calcium channels (HVACCs).[21] The Ca^{2+} current remaining after blockade of HVACC can then be studied in isolation from other Ca^{2+} currents.

The purpose of this study was to characterize pharmacologically isolated LVACC after neuropathic injury compared to sham-operated rats using fluorescent markers to identify cells with axons projecting to the injury site. An examination of this current provides information about the contribution of LVACC to total Ca^{2+} current in neuropathic signaling and reveals a role for LVACC in clinically observed chronic pain. Measurements were also made of the possible contribution of LVACC to membrane excitability. Some of these results have been presented in abstract form.[22]

Materials and Methods

Animal Preparation

As previously reported in detail, we used a CCI model of rat peripheral neuropathy for our studies.[19] Briefly, after Animal Resource Center approval, the right sciatic nerves of 175- to 200-g male rats anesthetized with halo-

* Research Scientist, † Assistant Professor, § Professor, Department of Anesthesiology, Medical College of Wisconsin. ‡ Associate Professor, Marquette University Department of Biology. ‖ Professor, Department of Anesthesiology, Medical College of Wisconsin, and VA Medical Center.

Received from the Department of Anesthesiology, Medical College of Wisconsin, Milwaukee, Wisconsin; Marquette University Department of Biology, Milwaukee, Wisconsin; and the VA Medical Center, Milwaukee, Wisconsin. Submitted for publication April 19, 2002. Accepted for publication September 3, 2002. Supported in part by the Research Affairs Committee Institutional Grant for Established Investigators, Medical College of Wisconsin, Milwaukee, Wisconsin, and Public Health Service Grant No. R01 NS42150-01 from the National Institutes of Health, National Institute of Neurological Disorders and Stroke, Rockville, Maryland.

Address reprint requests to Dr. McCallum: Department of Anesthesiology, Medical College of Wisconsin, 8701 Watertown Plank Road, Milwaukee, Wisconsin 53226. Address electronic mail to: mccallum@mcw.edu. Individual article reprints may be purchased through the Journal Web site, www.anesthesiology.org.

thane were ligated with four loosely tied 4-0 chromic gut ligatures under halothane anesthesia.[23] Sham rats received the same surgical exposure of sciatic nerve, but no ligatures were placed. The left leg of both groups remained intact for comparison to the operated side. To allow for determination of which neuronal somata projected axons to the sciatic nerve operative site, fluorescing DiI (1,1'-dioctadecyl-3,3,3',3'-tetramethylindocarbocyanine perchlorate) crystals were placed on the sciatic nerve and enclosed in a silicone rubber membrane (0.005 in; Technical Products, Inc., Decatur, GA) to prevent absorption of the dye into surrounding muscle. Ten days after surgery, we tested the rats for behavioral symptoms of hyperalgesia and allodynia. Briefly, rats were placed on a prewarmed glass surface, and their feet were exposed to a focused beam of incandescent heat with an infrared timer to detect paw withdrawal. Only rats with hind paw withdrawal latency less than 1.5 s shorter on the ipsilateral side compared to the contralateral side were included in the study. In addition, response to nociceptive mechanical stimulation in the plantar region of the hind paw was measured by indenting the skin with the point of a 22-gauge spinal needle. A normal response was a brief (nominally 0.5 s) withdrawal, whereas neuropathic response involved sustained elevation of the foot. In all, a neuropathic pain state was confirmed in approximately 50% of injured animals that exhibited a positive response to both these behavioral tests.

Our previous findings[19] and other published reports[16] suggest that pronounced T-type currents are primarily found in the medium-sized cells (33–42 μm) representing the nociceptors with Aδ lightly myelinated axons.[24] Therefore, only medium cells were used in this study.

Cell Isolation

The L4 and L5 DRG were removed from rats after halothane anesthesia and decapitation. To retard necrotic degradation, the spinal cord was perfused with cold, oxygenated rodent Ringer's solution consisting of 146 mM NaCl, 2 mM $CaCl_2$, 1 mM $MgCl_2$, and 1 mM HEPES through a spinal transection at the midsacral region. Ganglia were quickly removed and bathed in piperazine-*N,N'*-bis (2-ethanesulfonic acid) (PIPES)–buffered saline composed of 120 mM NaCl, 5 mM KCl, 1 mM $CaCl_2$, 1 mM $MgCl_2$, 25 mM d-glucose, and 20 mM PIPES. Excised ganglia were segmented with iris scissors to assist enzymatic digestion. Minced ganglia were transferred with silicone-coated Pasteur pipettes into 25-ml tissue culture flasks for shaking in enzyme solution containing 0.016% liberase blendzyme 2 (Roche Diagnostics Corp., Indianapolis, IN), 0.04% trypsin (Boehringer Mannheim, Mannheim, Germany), and 0.01% deoxyribonuclease 1 (150,000 U; Sigma, St. Louis, MO) in 5 ml oxygenated PIPES-buffered saline at a pH of 7.4 for 35–40 min at 150 rev/min. After complete dissociation was confirmed microscopically, cells were centrifuged at 778*g* for 6 min. The supernatant was removed, and cells were resuspended in a culture medium consisting of 0.5 mM glutamine, 0.02 mg/ml gentamicin, 100 ng/ml nerve growth factor 7S (Alomone Labs, Jerusalem, Israel), 2% (v/v) B-27 supplement (Life Technologies, Rockville, MD), and 98% (v/v) neurobasal medium A 1X (Life Technologies) before plating onto 12-mm poly-L-lysine–coated glass coverslips (Deutsche Spiegelglas; Carolina Biologic Supply, Burlington, NC). Coverslips were placed in a 12-well cell culture cluster and stored in a water-jacketed, humidified incubator at 37°C with 95% air and 5% CO_2. All cells were studied 6–8 h after dissociation.

Solutions

To isolate LVA from HVA I_{Ca}, cells were preincubated for at least 30 min in an external Tyrode's solution of the following composition: 140 mM NaCl, 4 mM KCl, 2 mM $CaCl_2$, 10 mM d-glucose, 2 mM $MgCl_2$, 10 mM HEPES, 0.001 mM ω-conotoxin (CTx) GVIA, and 0.002 mM ω-CTx MVIIC at a pH of 7.4 with NaOH and an osmolarity of 300 mOsM. ω-CTx GVIA irreversibly blocks N-type calcium channels, and ω-CTx MVIIC irreversibly blocks P-/Q-type calcium channels.[25–27] The concentrations used were saturating in preliminary experiments in this laboratory. Antagonist specificity was an issue in this study because no selective T-type Ca channel antagonist exists. Dihydropyridines were not used because they are known to block LVA Ca channels.[28] In addition to the irreversible block of HVA, the ω-CTxs used in this study reversibly block substantial amounts of LVA I_{Ca}. This was evident in control studies in which preincubated cells were subsequently exposed to either ω-CTx GVIA or MVIIC applied in the bath through a multibarreled microperfusion pipette placed 200 μm from the cell to determine sensitivity of the remaining current to acute administration. ω-CTx GVIA reduced current remaining after preincubation by 74%, while ω-CTx MVIIC reduced current by 86%, and these reductions were completely reversible. For this reason, ω-CTx was not used in the perfusion chamber during patch clamp studies. Any residual HVA I_{Ca} following incubation was eliminated by using fluoride in the internal pipette solution, which runs down HVA without reducing LVA I_{Ca}.[21,29,30] The efficacy of HVA rundown from fluoride was tested in six cells after preincubation in ω-CTx GVIA and equilibration with fluoride in the pipette. Application of 200 nM nisoldipine, a potent L-type channel blocker, in the bath had no effect on g_{max} (baseline = 1.5 ± 0.3 pS/pF *vs.* nisoldipine = 1.3 ± 0.2 pS/pF). Nickel sensitivity has been demonstrated for both R- and T-type LVA Ca channels.[27] In cells preincubated with ω-CTx, 10 μM Ni^{2+} reduced peak Ca channel conductance by 58.2 ± 1.6% in eight cells from neuropathic rats and 66.2 ± 0.02% in eight cells from sham rats (not significant). Ni^{2+} was

used as a marker for LVA I_{Ca} in current clamp studies only. The efficacy of pharmacological isolation of LVA I_{Ca} can be determined by comparison to our previous report of whole cell I_{Ca}.[19] In cells without ω-CTx or fluoride, peak I_{Ca} values were 3.06 ± 0.3 and 2.22 ± 0.26 pS/pF for cells from sham and neuropathic rats, respectively, more than three times the peak current reported in this study after pharmacological blockade.

The internal pipette solution consisted of 10 mM EGTA, 40 mM HEPES, 2 mM MgCl, an d135–140 mM tetramethylammonium hydroxide (TMA-OH) adjusted to a pH of 7.15–7.2 with hydrofluoric acid at an osmolarity of 290–300 mOsM. After preincubation, coverslips with their attached cells were transferred to the tissue chamber and perfused with an external solution designed to block potassium currents consisting of 152 mM TEA-Cl, 1 mM 4-aminopyridine (4-AP), 10 mM HEPES, and 5 mM $CaCl_2$ adjusted to a pH of 7.4 with TEA-OH at an osmolarity of 310–315 mOsM. The final TEA concentration was calculated at 165 mM. All solutions contained cytochrome *c* (0.1 mg/ml) to inhibit nonspecific protein binding.

Voltage Protocols

Only medium-sized cells demonstrating DiI fluorescence after excitation at 528–553 nm and emission between 577–632 nm were studied. Experiments were conducted at room temperature in the voltage or current clamp mode of the whole cell configuration of the patch clamp method using a List EP7 patch clamp amplifier (Adams List, Westbury, NY) connected to a personal computer through a Digidata 1200B digitizer (Axon Instruments, Union City, CA). Data were acquired at 5–50 kHz and filtered at 3 kHz with an eight-pole Bessel filter. The pClamp8 software suite (Axon Instruments) was used for data acquisition and analysis.

Experiments designed to characterize I_{Ca} began with an I-V protocol from a holding potential (V_H) of −100 mV. Leak current was subtracted *post hoc* by applying linear regression analysis to data points below current activation and then subtracting linear leak from the remainder of the I-V profile, provided that the linear fit passed through zero. Peak current amplitude was used in analyzing activation, inactivation, and deactivation protocols as described in relevant figure legends in the text. For determination of the dynamic characteristics of LVA current, two protocols were used. First, standard recovery from inactivation protocols employed a 1,000-ms conditioning pulse to inactivate channels followed by a test pulse of equal amplitude at increasing time intervals from 25 to 1,000 ms in 25-ms increments. Second, a ratio of sustained current (I_S) to peak current amplitude (I_P) was used to measure the rate of current inactivation. Specifically, late sustained current at the end of a 500-ms step protocol ranging from −100 mV to 10 mV was divided by early peak current at the same voltage. To approximate how I_{Ca} might respond to natural voltage stimulation, a voltage command in the form of an action potential (AP) waveform was employed, which was derived from an actual recorded AP in a medium-sized cell lasting 7 ms from a V_H of −68 mV. Another series of experiments was performed using current clamp mode in Tyrode's solution to determine the effect of T-type calcium channel blockade on excitability. Specifically, the amount of current necessary to evoke a single AP in a 20-ms step protocol was applied for 200 ms, and the number of APs were determined as a measure of neural excitability.

Statistical Analysis

Whole cell I_{Ca} was normalized to cell capacitance for comparison between cells. To characterize whole cell current, voltage dependence of I_{Ca} for each cell was fit to the following Boltzmann equation:

$$I = \frac{G_{max}\,(v - V_R)}{1 + \exp\,(v - V_{1/2}/k)}$$

where I is current, G_{max} is the maximum channel conductance, $V_{1/2}$ is the voltage at which current is half maximal, k is a slope factor describing voltage dependence of conductance, V_R is the reversal potential for current, and v is the membrane potential. Steady state activation and inactivation data were normalized to maximum current (I_{max}) or maximum conductance (g_{max}) and fit with a Boltzmann function with upper and lower confidence levels using Origin 6.0 (Microcal, Northampton, MA). Tail currents representing deactivation were easily fit to a single exponential function. The resulting time constants (τ) were averaged and described as a function of test potential. Average ratios of I_S *versus* I_P were plotted in studies of inactivation rate as a function of membrane potential in Origin and fit to a Boltzmann equation with upper and lower confidence levels. AP waveform data were normalized to cell capacitance and measured for peak inward current, area under the curve, half-width, and duration. Fitted parameters, central values, and AP waveform data were compared using Student *t* tests for unequal size between neuropathic and sham groups, and significance was determined at $P < 0.05$. Values expressed are mean ± SEM, unless otherwise noted.

Results

CCI injury produced a neuropathic state with clearly distinct behavioral characteristics compared to sham-operated rats. Sham rats had normal gait and paw appearance with an average nominal response latency of 0.5 s to punctate mechanical stimulation and an average latency of 7.0 ± 0.6 s to radiant heat. These were significantly different from neuropathic rats that dis-

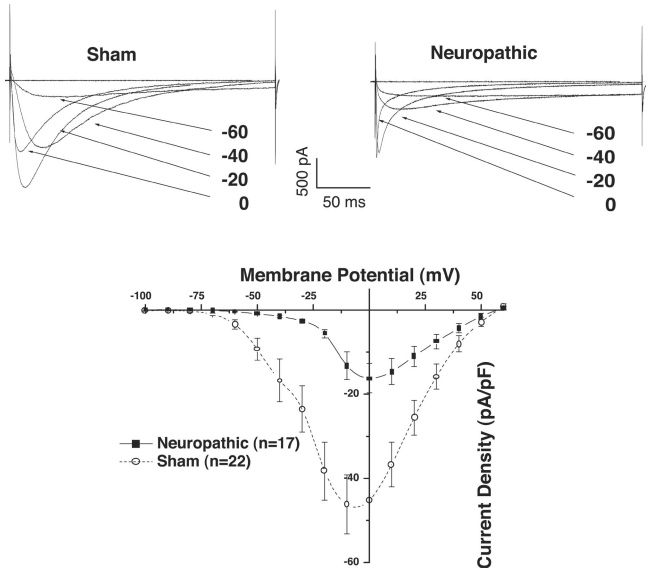

Fig. 1. Whole cell low-voltage–activated Ca^{2+} current (LVACC) was significantly reduced by neuropathic injury. Current remaining after preincubation with ωCtx GVIA or MVIIC and high-voltage–activated Ca^{2+} current rundown with Fl^- in the pipette was mostly LVACC (*inset*). Average peak inward current density was therefore fit to a single Boltzmann function (see text). Neuropathic cells exhibited a biphasic current profile with a small noninactivating current followed by a larger rapidly inactivating current. Maximum current density was decreased from 0.99 ± 0.44 pS/pF to 0.36 ± 0.07 pS/pF, and peak current activation was shifted 10 mV in a depolarizing direction.

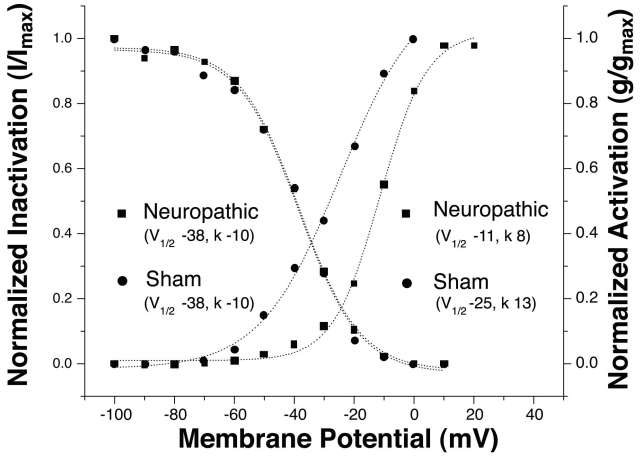

Fig. 2. The availability of LVA Ca channels after a preceding pulse was unchanged after neuropathy, but cells from neuropathic rats activated at more depolarizing potentials compared to cells from sham rats. The shift in activation reduced the overlap ("window current") between inactivation and activation, thereby attenuating total Ca^{2+} influx.

played protective behavior and deformed paw appearance accompanied by a delayed response to nociceptive mechanical stimulation and holding the paw aloft for 5.3 ± 0.8 s ($P < 0.01$) as well as an average heat withdrawal latency of 5.4 ± 0.8 s ($P < 0.05$). Mean cell diameter was 35.3 ± 0.8 μm with an average cell capacitance of 48.8 ± 3.7 pF. Sixty-nine cells from 26 rats, 15 sham and 11 neuropathic, were used in this study.

Whole cell I_{Ca} differed significantly between the two groups of cells (fig. 1 and table 1). Inward Ca^{2+} current in sham cells achieved peak activation at −10 mV where the conductance (g_{max}) was 0.99 ± 0.44 pS/pF, while current in neuropathic cells was maximally activated at 0 mV with a mean conductance of 0.36 ± 0.07 pS/pF. Current half-activation ($V_{1/2}$) was also significantly lower at −23 ± 3 mV for sham *versus* −12 ± 2 mV for neuropathic. Reversal potential (V_R) and the slope factors (k) were the same. Typical current traces (fig. 1, inserts) show how HVACC blockade in sham cells revealed a noninactivating current at extremely low voltages which gave way to a current at higher voltages with voltage-dependent rapid inactivation, a characteristic of T-type currents. Visible in neuropathic cells is a faster rate of inactivation at voltages generating peak currents compared to sham cells. Four of 17 neuropathic cells displayed characteristic T-type LVA Ca channels, while 16 of 22 sham cells exhibited currents with these features—a difference of $P = 0.004$ according to Fisher exact test for two-sided chi-square. Of the neuropathic cells lacking characteristic T current, 11 showed extremely short currents in which inactivation was not voltage dependent.

Table 1. Boltzmann Parameters for IV Curves

	Neuropathic Cells (n = 17)	Sham Cells (n = 22)
G_{max}, pS/pF	0.36 ± 0.07*	0.99 ± 0.44
V_R, mV	54 ± 2	51 ± 2
$V_{1/2}$, mV	−12 ± 2*	−23 ± 3
K, slope	−6.9 ± 0.9	−6.9 ± 0.08

*$P < 0.05$ *versus* sham.

G_{max} = conductance; IV curve = current *versus* voltage curve; K = slope factors; $V_{1/2}$ = current half-activation; V_R = reversal potential.

Various features of these currents, including voltage dependence and kinetics, differed between the sham and neuropathic groups. Neuropathic injury shifted the voltage dependence of activation in a depolarized direction (fig. 2). Activation was determined by dividing peak current by the driving force to determine chord conductance and expressed as proportion of peak conductance. Sham cells were half-activated at −25 ± 0.7 mV, while neuropathic cells became half-activated at −11 ± 0.7 mV ($P = 0.04$).

Steady state inactivation was measured in a conventional way by a 500-ms prepulse from V_H of −100 to 0 mV in 10-mV increments followed by a second test pulse to −10 mV. Results were normalized to peak current (fig. 2). One half of inward Ca^{2+} current was inactivated at −38 ± 0.7 mV in both the sham and neuropathic groups. Though voltage dependence of inactivation was unchanged by injury, the extent and kinetics of current inactivation were significantly different. Since macroscopic inactivation was immeasurably small at hyperpolarized potentials where current did not inac-

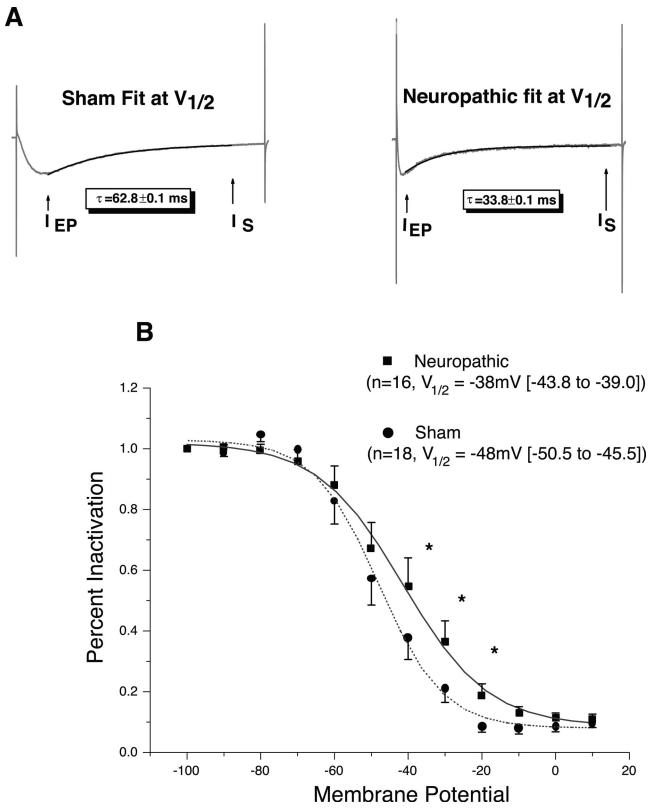

Fig. 3. The ratio of early peak (I_{EP}) to late sustained (I_S) current indicates that current inactivation during a stimulus pulse was greater in cells from neuropathic animals at command voltages from −50 to −20 mV. Extent of inactivation was more steeply voltage dependent in cells from sham rats. Half of peak current inactivated at −48 mV in sham *versus* −38 mV in neuropathic (upper and lower confidence levels in brackets). The rate of inactivation was faster in cells from neuropathic rats (examples in insets). When the actual wave data from the traces where 50% of the current was inactivated were fit to a single exponential, average inactivation rates were significantly faster (τ = 186 ± 32 ms) for neuropathic compared to sham cells (τ = 268 ± 36 ms).

tivate, a ratio of current at early peak (I_{EP}) to sustained current (I_S) was used to examine the extent of LVA Ca^{2+} current inactivation (fig. 3). Inactivation was greater in neuropathic cells at voltages of −50 to −20 mV. At −48 (−51 LCL to −46 UCL) mV, sham I_{Ca} was 50% inactivated at the end of a 500-ms test pulse, while neuropathic I_{Ca} was 50% inactivated at −38 (−44 LCL to −39 UCL) mV. The extent of inactivation was more steeply voltage dependent in sham *versus* neuropathic cells (fig. 3A, fig. 1 insert). Voltage differences in the ratio reflect higher peak conductance at lower membrane potentials, but they do not indicate the kinetics of channel inactivation. To estimate these rates, the trace at voltages showing 50% inactivation was fit to a single exponential for each cell. Neuropathic cells were 50% inactivated significantly faster at (τ = 186 ± 32 ms, n = 16) compared to sham cells (τ = 268 ± 36 ms, n = 18, fig. 3B). These significant differences in extent and pace of inactivation did not affect time to recover from inactivation (fig. 4). Recovery from inactivation for both

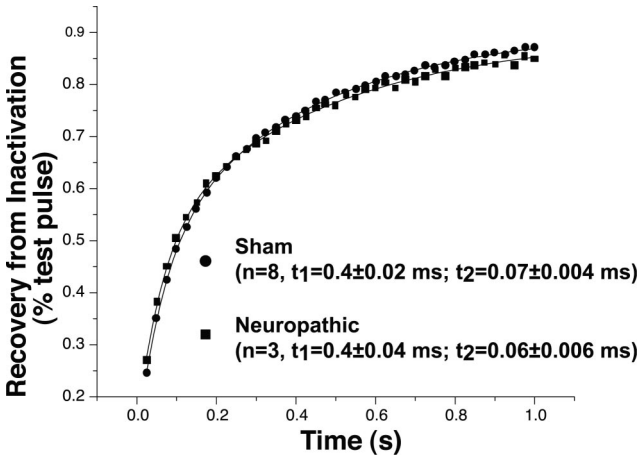

Fig. 4. Recovery from inactivation was the same for both groups. The interval between prepulse and test pulse was gradually prolonged until peak current resembled current at test.

groups was easily fit by a two-exponential nonlinear function with τ_{fast} = 409 ± 22 ms; τ_{slow} = 68 ± 4 ms for sham and τ_{fast} = 447 ± 45 ms; τ_{slow} = 64 ± 6 ms (not significant) for neuropathic.

Since T-type Ca^{2+} currents deactivate (revert to nonconducting state upon repolarization) slowly, tail current kinetics were measured after a 20-ms depolarizing prepulse to a voltage that achieves peak activation followed by a return to test potentials ranging from −10 mV to −100 mV. Figure 5 shows a family of tail currents with the typical pattern of T-type Ca channel relaxation. Tail currents were fit by a single exponential, and the time constant of deactivation, τ, was plotted

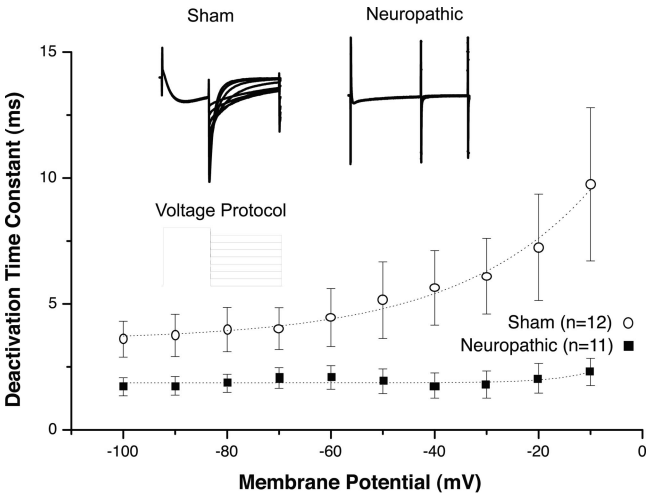

Fig. 5. Deactivation rates for sham were significantly slower than neuropathic. Cells were exposed to a 20-ms prepulse to maximal activation followed by test pulses in gradually more hyperpolarized direction until tail currents demonstrated an almost instantaneous relaxation of current. Tail currents were fit to a single exponential function to derive a τ of deactivation. The normal crossing pattern of deactivation was present in sham cells indicating a voltage dependence of τ, whereas neuropathic cells recovered almost instantaneously from current activation at all voltages.

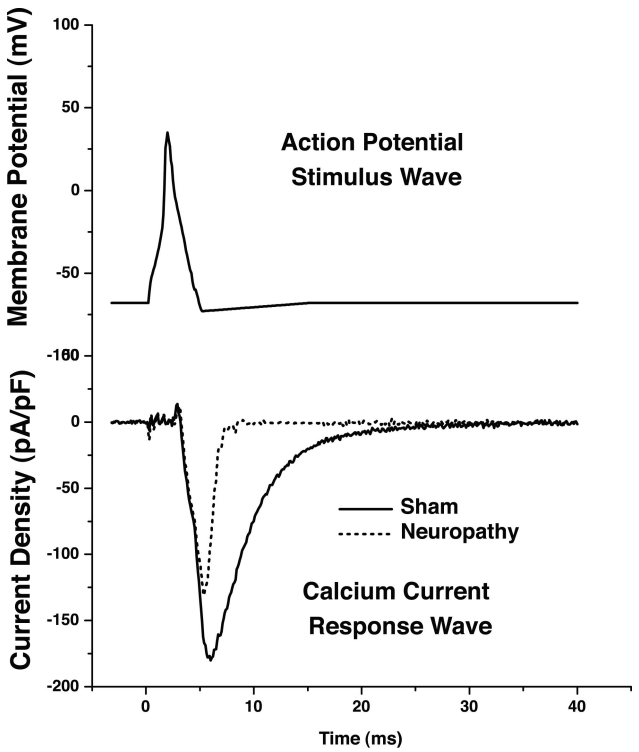

Fig. 6. Whole cell LVA Ca^{2+} flux was significantly reduced in cells from neuropathic rats compared to sham. In response to an action potential (AP) waveform, peak current density declined from −45.2 ± 13.4 pA/pF (n = 21) to −20.1 ± 4.6 pA/pF (n = 16) after neuropathy, and the area under the wave representing total Ca^{2+} flux dropped from −199.6 ± 91.4 pA/pF to −40.4 ± 5.7 pA/pF · ms after neuropathy. Likewise, duration of Ca^{2+} flux was reduced from 9.9 ± 1.3 ms to 5.2 ± 0.4 ms.

against membrane potential. Deactivation was clearly voltage dependent in sham cells where the decay curve was nicely fit by an exponential function, whereas deactivation was not voltage dependent in neuropathic cells in which time constants for deactivation within the range of test potentials were easily associated with a linear function.

Neuropathy significantly reduced Ca^{2+} current in response to an AP voltage command waveform (fig. 6). Peak current density dropped from −45.2 ± 13.4 pA/pF (n = 21) to −20.1 ± 4.6 pA/pF (n = 16) after neuropathy, and the area under the wave representing total Ca^{2+} charge flux declined from 199.6 ± 91.4 pA/pF to 40.4 ± 5.7 pA/pF · ms after neuropathy. Likewise, duration of Ca^{2+} current flux was reduced from 9.9 ± 1.3 ms to 5.2 ± 0.4 ms by neuropathy, and half-width declined from 2.5 ± 0.2 ms to 1.5 ± 0.1 ms.

Blockade of LVA Ca^{2+} current with low concentrations of Ni^{2+} or mibefradil enhanced neuronal excitability and decreased inward current in uninjured cells (fig. 7). Five micromolar Ni^{2+} increased the frequency of APs twofold in response to a 200-ms ramped current injection, and this effect was reversible on washout. The presumption that this was due to Ca^{2+} channel blockade is supported by the simultaneous decrease in inward current, which was reversed on washout. It is known that Ni^{2+} also blocks Na^+ currents, but decreased I_{Na} would be expected to decrease spike initiation rather than increase it. In another series using 300 nM mibefradil, a potent LVA Ca^{2+} channel blocker with an EC_{50} of 3 μM, the frequency of APs evoked in response to a 200-ms ramp pulse rose significantly from 3.4 ± 0.9 (n = 7) to 6 .5 ± 0.8 (n = 6), while peak inward current significantly declined from 319 ± 49 pS/pF to 160 ± 77 pS/pF at a V_{test} of −10 mV (data not shown).

Discussion

This study of the effect of neuropathic injury on LVA I_{Ca} in rat DRG cells shows that low-voltage–activated calcium currents are significantly reduced after CCI of the peripheral nerve. The cause of this reduction appears to be a decrease in current density, a depolarizing shift in the voltage dependence of activation, an increase in the rate of deactivation, and more rapid and extensive inactivation. Even though I_{Ca} in neuropathic cells was activated at more positive membrane potentials, there was no change in voltage dependence of channel availability as shown by the steady state inactivation curves. The shift in activation after neuropathy also diminished the window current seen in the overlap of inactivation and activation curves of sham cells. The combined effect of these changes was observed in response to an AP waveform. Depressed Ca^{2+} influx is shown by reduced area under the curve in neuropathic cells as well as diminished peak current, and accelerated deactivation

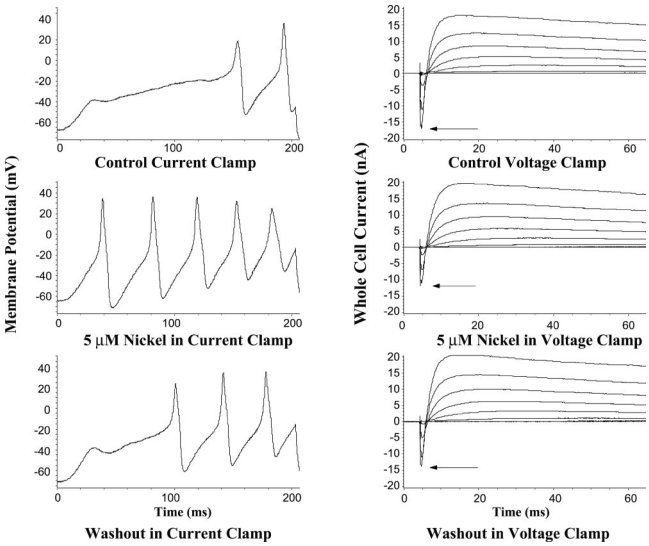

Fig. 7. Ni^{2+} added to the superfusate of this cell recorded in current clamp mode increased excitability by mimicking the loss of Ca^{2+} after neuropathy. The frequency of action potentials in response to current injection ramped over 200 ms from 0 to 2.5 nA was increased by 5 μM Ni^{2+} in the superfusate and reversed by washout, while the same cell in voltage clamp displayed a loss of inward Ni^{2+}-sensitive current (*arrows*).

appears in the shorter duration of I_{Ca} in response to a physiologically relevant command. Since LVA activity cannot be isolated during current clamp protocols, the contribution of LVA Ca^{2+} current to membrane excitability was mimicked by administration of low-dose Ni^{2+} or mibefradil to the cell in current clamp mode. Both mibefradil and Ni^{2+} increased the firing frequency in response to a 200-ms current injection.

The origin of neuropathic pain after peripheral trauma or pathology is complex. Ectopic discharge in DRG somata of hyperalgesic rats has been implicated.[7] However, the number of spontaneously active cells constitutes a small portion of all cells recorded in DRGs from neuropathic animals.[31] Sympathetic sprouting into the DRG, accompanying Wallerian degeneration, also contributes to excitability in models of painful neuropathy,[32–35] although the cells in our experiments were free from adrenergic inputs. Another physiologic response to injury is the phenomenon of cross-excitation, whereby spontaneously active or hyperexcitable cells can recruit adjacent cells, possibly through intercellular K^+ accumulation.[36] Recent evidence suggests, however, that critical changes take place in pain by which cellular and chemical modifications cause primary sensory neurons to spontaneously discharge or oscillate secondary to mechanical stimulation.[13,37]

The cellular mechanisms of enhanced excitability are poorly understood. Widely reported changes in the expression of various Na channel subtypes suggest that faster spike initiation would presumably increase excitability. It is known that fast-activating, TTX-sensitive Na channels are overexpressed and slower-activating, TTX-resistant channels are underexpressed in sensory neurons after injury.[38] Regardless of the initiation of neuronal activity, afferent signaling is ultimately limited by the ability of the sensory neuron to fire repetitively. Inward Ca^{2+} current decreases neuronal firing rates by opening Ca-activated K channels, which make the cell less excitable. When Ca^{2+} current is reduced, the cell becomes less stable and more excitable.[39–43]

Low-voltage–activated Ca^{2+} currents have been implicated in rebound burst firing in thalamic relay neurons and cerebellar Purkinje cells associated with epilepsy[44] and pacemaker activity in the upper heart.[45] However, the role of LVA Ca^{2+} currents in primary afferent neurons is unknown. One study in the DRG disclosed a rebound triggering mechanism,[17] in which LVA currents are de-inactivated at very negative potentials and subsequently opened during return to resting membrane potential, admitting an inward current. However, the extreme hyperpolarization used in that study to produce this response is not characteristic of sensory neurons, and the very short (1- to 5-mS) duration of sensory neuron APs results in minimal channel inactivation. It is more likely, rather, that the role of T currents in primary afferent neurons, as a conduit of substantial Ca^{2+} entry,[46] is due to slow deactivation at the end of an AP, at which time the driving force on Ca^{2+} ions is also very large.[46] Absence of this prolonged Ca^{2+} influx in injured neurons would contribute to increased excitability.[47] Of course, in the central nervous system, the role of LVACC may be entirely different.

Not all neuropathic cells were without T-type Ca^{2+} current in our study, nor was it fully expressed in all sham cells. Indeed, several features of currents in our cells differ from published reports of LVA Ca^{2+} current. For example, the midpoints of activation were -25 mV in our sham cells compared to -36 ± 0.5 mV in systems expressing only α_1 subunits without auxiliary β or δ subunits.[48] However, despite the difference in LVA Ca^{2+} current profile in these cells, a significant loss of LVA Ca^{2+} current accompanied neuropathic injury.

The current that remained after injury was not due to Ca^{2+} passing through TTX-insensitive Na channels because the remainder current was sensitive to the Ca channel blockers Cd^{2+} (data not shown) and Ni^{2+}. Furthermore, 160 mM TEA and 1 μM TTX were present in the external solution to substitute for Na^+ and block the TTX-sensitive Na channels, respectively. A more likely explanation for the remainder current in neuropathic cells involves the newly recognized heterogeneity of LVA Ca channels. Of the three subtypes, $\alpha 1_G$, $\alpha 1_H$, and $\alpha 1_I$, only $\alpha 1_H$ and $\alpha 1_I$ are differentially expressed in the DRG, according to *in situ* hybridization examination.[49] The $\alpha 1_I$ subtype inactivates more slowly than $\alpha 1_H$,[50] which corresponds to earlier observations of fast- and slowly inactivating T-current subtypes.[51,52] It would therefore appear that the slowly activating $\alpha 1_I$ subtype is preferentially inhibited by nerve injury, leaving intact a faster-inactivating $\alpha 1_H$, although the exact nature of the remainder current has yet to be determined.

Other studies of Ca^{2+} currents in the DRG of neuropathic rats found decreases in whole cell Ca^{2+} current, but they did not observe differences in the number of cells with detectable LVA Ca^{2+} currents in sham *versus* neuropathic groups.[20,53] However, these studies did not specifically isolate T-currents with pharmacological agents. Furthermore, these studies either selectively studied identified cutaneous neurons[20] or nonselectively examined injured and noninjured neurons.[53] Deep, persistent pain characterized by hyperalgesia and allodynia preferentially arises from muscle afferents that become spontaneously active after nerve injury. We labeled more proximally at the sciatic nerve injury site, which means that both muscle and cutaneous afferents were included.

In sum, neuropathy sharply reduces inward current through LVA calcium channels of sensory neurons by shifting the voltage dependence of activation in a more depolarized direction, reducing calcium conductance and increasing the extent and rate of inactivation. These changes are reflected in a decreased total calcium current induced by a virtual AP waveform in injured neu-

rons. Mimicking this loss by addition of low micromolar nickel or mibefradil produces a reversible increase in neuronal excitability. Future studies in nondissociated DRG tissue and intact neuropathic rats will be necessary to determine whether this loss of Ca^{2+} current is responsible for increased excitability.

The authors thank Rich Rys (Senior Research Engineer, Department of Anesthesiology, Medical College of Wisconsin, Milwaukee, Wisconsin) for his valuable engineering help.

References

1. Woolf CJ: Somatic pain: Pathogenesis and prevention. Br J Anaesth 1995; 75:169–76
2. Gold MS: Spinal nerve ligation: What to blame for the pain and why. Pain 2000; 84:117–20
3. Devor M, Seltzer Z: Pathophysiology of damaged nerves in relation to chronic pain, Textbook of Pain, 4th edition. Edited by Wall PD, Melzack R. Edinburgh, Churchill Livingstone, 1999, pp 29–164
4. Thompson SW, Woolf CJ, Sivilotti LG: Small-caliber afferent inputs produce a heterosynaptic facilitation of the synaptic responses evoked by primary afferent A-fibers in the neonatal rat spinal cord in vitro. J Neurophysiol 1993; 69:2116–28
5. Kirk EJ: Impulses in dorsal spinal nerve rootlets in cats and rabbits arising from dorsal root ganglia isolated from the periphery. J Comp Neurol 1974; 155:165–75
6. Wall PD, Devor M: Sensory afferent impulses originate from dorsal root ganglia as well as from the periphery in normal and nerve injured rats. Pain 1983; 17:321–39
7. Kajander KC, Wakisaka S, Bennett GJ: Spontaneous discharge originates in the dorsal root ganglion at the onset of a painful peripheral neuropathy in the rat. Neurosci Lett 1992; 138:225–8
8. Study RE, Kral MG: Spontaneous action potential activity in isolated dorsal root ganglion neurons from rats with a painful neuropathy. Pain 1996; 65:235–42
9. Han H, Lee D, Chung J: Characteristics of ectopic discharges in a rat neuropathic pain model. Pain 2000; 84:253–61
10. Liu CN, Wall PD, Ben-Dor E, Michaelis M, Amir R, Devor M: Tactile allodynia in the absence of C-fiber activation: Altered firing properties of DRG neurons following spinal nerve injury. Pain 2000; 85:503–21
11. Liu X, Eschenfelder S, Blenk KH, Janig W, Habler H: Spontaneous activity of axotomized afferent neurons after L5 spinal nerve injury in rats. Pain 2000; 84:309–18
12. Amir R, Devor M: Spike-evoked suppression and burst patterning in dorsal root ganglion neurons of the rat. J Physiol 1997; 501:183–96
13. Liu CN, Michaelis M, Amir R, Devor M: Spinal nerve injury enhances subthreshold membrane potential oscillations in DRG neurons: relation to neuropathic pain. J Neurophysiol 2000; 84:205–15
14. Miletic G, Miletic V: Long-term changes in sciatic-evoked A-fiber dorsal horn field potentials accompany loose ligation of the sciatic nerve in rats. Pain 2000; 84:353–9
15. Scroggs RS, Fox AP: Calcium current variation between acutely isolated adult rat dorsal root ganglion neurons of different size. J Physiol 1992; 445: 639–58
16. Scroggs RS, Fox AP: Multiple Ca^{2+} currents elicited by action potential waveforms in acutely isolated adult rat dorsal root ganglion neurons. J Neurosci 1992; 12:1789–801
17. White G, Lovinger DM, Weight FF: Transient low-threshold Ca^{2+} current triggers burst firing through an afterdepolarizing potential in an adult mammalian neuron. Proc Natl Acad Sci U S A of the United States of America 1989; 86:6802–6
18. Tsakiridou E, Bertollini L, de Curtis M, Avanzini G, Pape HC: Selective increase in T-type calcium conductance of reticular thalamic neurons in a rat model of absence epilepsy. J Neurosci 1995; 15:3110–7
19. Hogan QH, McCallum JB, Sarantopoulos C, Aason M, Mynlieff M, Kwok WM, Bosnjak ZJ: Painful neuropathy decreases membrane calcium current in mammalian primary afferent neurons. Pain 2000; 86:43–53
20. Baccei ML, Kocsis JD: Voltage-gated calcium currents in axotomized adult rat cutaneous afferent neurons. J Neurophysiol 2000; 83:2227–38
21. Todorovic SM, Lingle CJ: Pharmacological properties of t-type Ca^{2+} current in adult rat sensory neurons: Effects of anticonvulsant and anesthetic agents. J Neurophysiol 1998; 79:240–52
22. McCallum JB, Kwok WM, Bosnjak ZJ, Hogan QH: Neuropathic injury reduces T-type calcium current but not R-type in rats. Soc Neurosci Abstracts 2000; 26(pt 1):893
23. Bennett GJ, Xie YK: A peripheral mononeuropathy in rat that produces disorders of pain sensation like those seen in man. Pain 1988; 33:87–107
24. Harper AA, Lawson SN: Conduction velocity is related to morphological cell type in rat dorsal root ganglion neurones. J Physiol 1985; 359:31–46
25. Nooney JM, Lodge D: The use of invertebrate peptide toxins to establish Ca^{2+} channel identity of CA3-CA1 neurotransmission in rat hippocampal slices. Eur J Pharmacol 1996; 306:41–50
26. Randall A, Tsien RW: Pharmacological dissection of multiple types of Ca^{2+} channel currents in rat cerebellar granule neurons. J Neurosci 1995; 15:2995–3012
27. Tottene A, Volsen S, Pietrobon D: Alpha(1E) subunits form the pore of three cerebellar R-type calcium channels with different pharmacological and permeation properties. J Neurosci 2000; 20:171–8
28. Richard S, Diochot S, Nargeot J, Baldy-Moulinier M, Valmier J: Inhibition of T-type calcium currents by dihydropyridines in mouse embryonic dorsal root ganglion neurons. Neurosci Lett 1991; 132:229–34
29. Kostyuk PG, Krishtal OA, Pidoplichko VI: Effect of internal fluoride and phosphate on membrane currents during intracellular dialysis of nerve cells. Nature 1975; 257:691–3
30. Carbone E, Lux HD: Kinetics and selectivity of a low-voltage-activated calcium current in chick and rat sensory neurones. J Physiol 1987; 386:547–70
31. Song XJ, Hu SJ, Greenquist KW, Zhang JM, LaMotte RH: Mechanical and thermal hyperalgesia and ectopic neuronal discharge after chronic compression of dorsal root ganglia. J Neurophysiol 1999; 82:3347–58
32. McLachlan EM, Jang W, Devor M, Michaelis M: Peripheral nerve injury triggers noradrenergic sprouting within dorsal root ganglia. Nature 1993; 363: 543–6
33. Petersen M, Zhang J, Zhang JM, Lamotte RH: Abnormal spontaneous activity and responses to norepinephrine in dissociated dorsal root ganglion cells after chronic nerve constriction. Pain 1996; 67:391–7
34. Devor M, Janig W, Michaelis M: Modulation of activity in dorsal root ganglion neurons by sympathetic activation in nerve-injured rats. J Neurophysiol 1994; 71:38–47
35. Ramer MS, French GD, Bisby MA: Wallerian degeneration is required for both neuropathic pain and sympathetic sprouting into the DRG. Pain 1997; 72:71–8
36. Shinder V, Devor M: Structural basis of neuron-to-neuron cross-excitation in dorsal root ganglia. J Neurocytol 1994; 23:515–31
37. Ma QP, Woolf CJ: Progressive tactile hypersensitivity: An inflammation-induced incremental increase in the excitability of the spinal cord. Pain 1996; 67:97–106
38. Cummins TR, Waxman SG: Downregulation of tetrodotoxin-resistant sodium currents and upregulation of a rapidly repriming tetrodotoxin-sensitive sodium current in small spinal sensory neurons after nerve injury. J Neurosci 1997; 17:3503–14
39. Adams PR, Galvan M: Voltage-dependent currents of vertebrate neurons and their role in membrane excitability. Adv Neurol 1986; 44:137–70
40. Harper AA: Similarities between some properties of the soma and sensory receptors of primary afferent neurones. Exp Physiol 1991; 76:369–77
41. Vergara C, Latorre R, Marrion NV, Adelman JP: Calcium-activated potassium channels. Curr Opin Neurobiol 1998; 8:321–9
42. Everill B, Kocsis JD: Reduction in potassium currents in identified cutaneous afferent dorsal root ganglion neurons after axotomy. J Neurophysiol 1999; 82:700–8
43. Lüscher C, Lipp P, Lüscher HR, Niggli E: Control of action potential propagation by intracellular Ca^{2+} in cultured rat dorsal root ganglion cells. J Physiol 1996; 490:319–24
44. Huguenard JR: Low-threshold calcium currents in central nervous system neurons. Annu Rev Physiol 1996; 58:329–48
45. Cribbs LL, Lee JH, Yang J, Satin J, Zhang Y, Daud A, Barclay J, Williamson MP, Fox M, Rees M, Perez-Reyes E: Cloning and characterization of alpha1H from human heart, a member of the T-type Ca^{2+} channel gene family. Circ Res 1998; 83:103–9
46. McCobb DP, Beam KG: Action potential waveform voltage-clamp commands reveal striking differences in calcium entry via low and high voltage-activated calcium channels. Neuron 1991; 7:119–27
47. Hogan Q, McCallum J, Seagard J: Blockade of Ca^{2+} current excites dorsal root ganglion (DRG) neurons. Soc Neurosci Abstracts 2000; 26:893
48. Perez-Reyes E: Molecular characterization of a novel family of low voltage-activated, T-type, calcium channels. J Bioenerg Biomembr 1998; 30:313–8
49. Talley EM, Cribbs LL, Lee JH, Daud A, Perez-Reyes E, Bayliss DA: Differential distribution of three members of a gene family encoding low voltage-activated (T-type) calcium channels. J Neurosci 1999; 19:1895–911
50. Lee JH, Daud AN, Cribbs LL, Lacerda AE, Pereverzev A, Klockner U, Schneider T, Perez-Reyes E: Cloning and expression of a novel member of the low voltage-activated T-type calcium channel family. J Neurosci 1999; 19:1912–21
51. Dolphin AC: Properties and modulation of T-type currents in dorsal root ganglia and ND7-23 cell: Comparison with α_{1E} currents expressed in COS-7 cells, Low-voltage-activated T-type Calcium Channels: Proceedings from the International Electrophysiology Meeting, Montpellier, October 21–22, 1996. Edited by Tsien RW, Closel J-P, Nargeot J. Chester, United Kingdom, Adis International Limited, 1998, pp 269–78
52. Tarasenko AN, Kostyuk PG, Eremin AV, Isaev DS: Two types of low-voltage-activated Ca^{2+} channels in neurones of rat laterodorsal thalamic nucleus. J Physiol 1997; 499:77–86
53. Abdulla FA, Smith PA: Axotomy- and autotomy-induced changes in Ca^{2+} and K^+ channel currents of rat dorsal root ganglion neurons. J Neurophysiol 2001; 85:644–58